

## [Supplementary material]

### Dating Mediterranean shipwrecks: the Mazotos ship, <sup>14</sup>C, and the need for independent chronological anchors

Sturt W. Manning<sup>1,2,\*</sup>, Brita Lorentzen<sup>1</sup> & Stella Demesticha<sup>3,\*</sup>

<sup>1</sup> Cornell Tree Ring Laboratory, Department of Classics, Cornell University, USA

<sup>2</sup> The Cyprus Institute, Nicosia, Cyprus

<sup>3</sup> Archaeological Research Unit, Department of History and Archaeology, University of Cyprus, Nicosia, Cyprus

\* Author for correspondence ✉ sm456@cornell.edu, demesticha@ucy.ac.cy

#### Example amphorae from the Mazotos ship

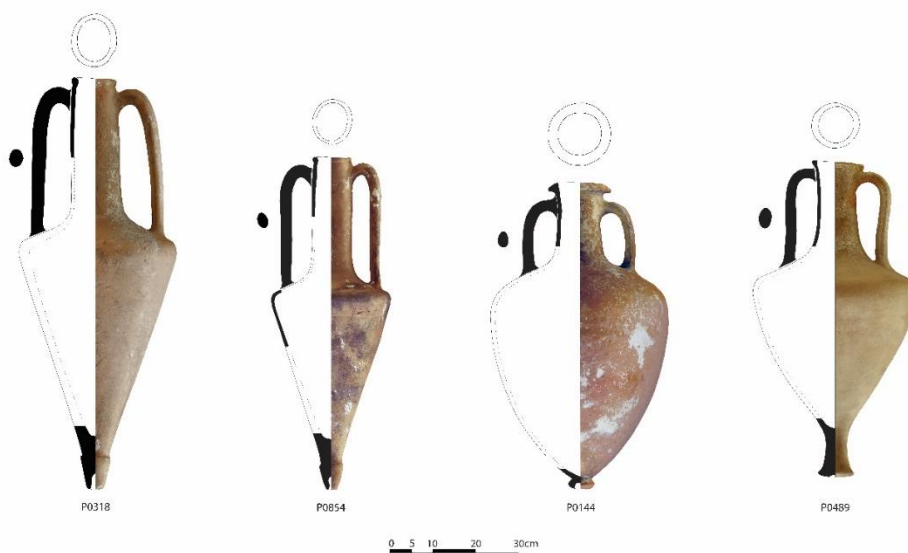


*Figure S1. Characteristic cargo amphorae from the Mazotos shipwreck. From left to right: Chian (large and small size); Mushroom-rim/Solokha I; and North Aegean (drawings: A. Evripidou; photography: M. Secci).*

#### Additional information on samples, and dating considerations in the Mazotos chronological model

The W0056/3 *Pinus nigra* sample, from a plank cut (#W0056) from the stern area of the Mazotos ship (Figure S2) and used for the radiocarbon wiggle-match is shown in Figure S3. Examples of the more than 1100 twig fragments used for dunnage (#W0051) that were found on top of the planking preserved at the Mazotos ship's stern are shown in Figure S4. A

considerable number of olive pits were recovered. For example, in total more than 2500 olive pits (#G0362) were found inside a broken Chian amphora, stowed in the aft part of the Mazotos ship's hold (Figure S5). Some of these were dated (see Table S1).



*Figure S2. The exposed part of the Mazotos stern, where a planking section was sampled for dendrochronology; white box: the strake from which #W0056 was cut (photograph: A. Kritiotis).*



Figure S3. Cross section of W0056, a *Pinus nigra* plank (sample #W0056/3) from the stern area of the Mazotos ship, showing the tree's pith and tree-rings out to the last extant tree-ring (RY 1047) (photograph: B. Lorentzen).



Figure S4. Subsample of more than 1100 twig fragments used for dunnage (#W0051) found on top of the planking preserved at the Mazotos ship's stern. The yellow label tag is approximately 75mm wide (left to right) (photograph: I. Katsouri).



Figure S5. More than 2500 olive pits (#G0362) were found inside a broken Chian amphora, stowed in the aft part of the Mazotos ship's hold (photograph: S. Demesticha).

### Missing rings

Examination of the cross-section of plank W0056 used in the  $^{14}\text{C}$  wiggle-match in our chronological model shows that both the tree's pith (located at the center of the stem) and wide juvenile rings are present, meaning that the plank contains the innermost/least recent tree-rings of the tree from which it was cut. From both the sample's anatomical features (pith and juvenile rings, along with lack of bark/waney edge) and condition (multiple teredo worm holes and decay), it is clear that the last extant tree ring on the plank (Relative Year (RY) 1047) is not the original outermost tree-ring. Instead, an unknown number of rings are missing between RY 1047 and the original tree trunk's outermost, most recent ring (waney edge) underneath the bark. There could easily be several to a larger number of tree-rings missing. We consider models with 0, 5, 10, 20, 40, 50 and 60 possible missing rings (see Figures S6–S7). We also include a possible growing season adjustment applied to the two Lamiaceae twigs (see below) since this would likely (very slightly) maximise any difference between *Pinus nigra* TPQ and Lamiaceae LV date. We stop at approximately 60 missing rings because the quality of the wiggle-match fit deteriorates with larger values. The first tree-ring sample, VERA-6299B MAZS-1 W0056/3 RY1005-1007, is an approximately 6%

probability outlier in the 0 to 20 missing rings models, but the individual agreement (A) value is satisfactory ( $\geq 60$ ). However, by the time we reach an assumption of 40 missing rings, the outlier probability has increased a little to approximately 7%, and the individual agreement value is now  $< 60$  at approximately 52.4%; at 50 missing rings it is a 9% outlier probability and A = approximately 41.9%; and by 60 missing rings it has 10% outlier probability and A = approximately 32.5%. Thus, it seems likely the correct number of missing rings is less than 60. Under each of the scenarios considered from 0 to 60 missing rings, the LV date does not really change (some examples are shown in Figure S6). The set of dates on the dunnage and the olive pits circumscribe the possible LV date given that the last ring of the ship timber must be plausibly close in time (that is: within decades and not, for example, a century or so earlier).

Our other relevant measure is the likely maximum ship service period (MSSP) calculated by each model (Figure S7). This—the maximum period possible—is the difference between the dates of the LV and of the last tree-ring on #W0056. We know, based on a range of ethnohistorical and archaeological evidence (e.g. Dodds & Moore 2005: 17; Pomey & Rieth 2005: 142; Manning *et al.* 2009; Lorentzen *et al.* 2014a: 776, 2014b), that the anticipated service period of traditional to pre-modern wooden ships is likely to be around on average  $\leq 20$ –30 years. Of course, there will be exceptions. Additional archaeological information or assessment of the specific ship's timbers may confirm or refine this basic assumption.

Without allowing for at least a few missing rings, as is already indicated as necessary from examining #W0056, the MSSP for the Mazotos ship tends towards the beyond average to long-lived. While possible, it can be observed that once we assume there are about 10 or 15 to 20 missing rings, then the MSSP becomes a more likely typical value (with 68.3% hpd ranges of 7–27, 3–19 and 2–16 years respectively; and 95.4% hpd ranges of 2–46, 1–38 and 1–36 years respectively) (see Figure S7). The maximum service period does not really change substantially thereafter across assumptions of approximately 20–60 missing rings (the wiggle-match date for #W0056 is merely pushed backwards as far as possible). Thus, the efficient and expedient solution would be to assume that approximately 10–20 rings are likely missing between the last extant tree ring of #W0056 (RY 1047) and what was the final ring under the bark in the original stem, whose date corresponds to the year the tree was felled and is likely within a year or two at most of the ship's construction date. This is because most evidence points to wood being used either immediately (green, when easy to work) or within a year (or two at most) in the pre-modern era in Europe and the Mediterranean basin—for example, timber was commonly felled after the end of the growing season in the autumn, for

use the following year. In between, it was allowed to dry (season). Of course, transport and stockpiling could lengthen the period between cutting and the ship's construction, relevant especially for larger projects (for some assessments and examples see, for example, Meiggs 1982: 125, 180 & 349–50; Kuniholm & Striker 1987; Büntgen *et al.* 2006; Miles 2006; Eckstein 2007; Crone & Mills 2012; Bernabei *et al.* 2019). Again, examining the ship timber anatomy and carpentry marks allows further assessment of these assumptions for the specific ship (Lorentzen *et al.* 2020). On-going examination of other timbers from the Mazotos ship, if they preserve additional tree rings beyond RY 1047 of #W0056, and especially the tree's bark and/or waney edge, may better indicate the real number of missing rings (in this case) and allow closer estimation of the construction date of the Mazotos ship in the future. However, as evident from Figures S6 and S7, this is very unlikely to change the date of the LV.

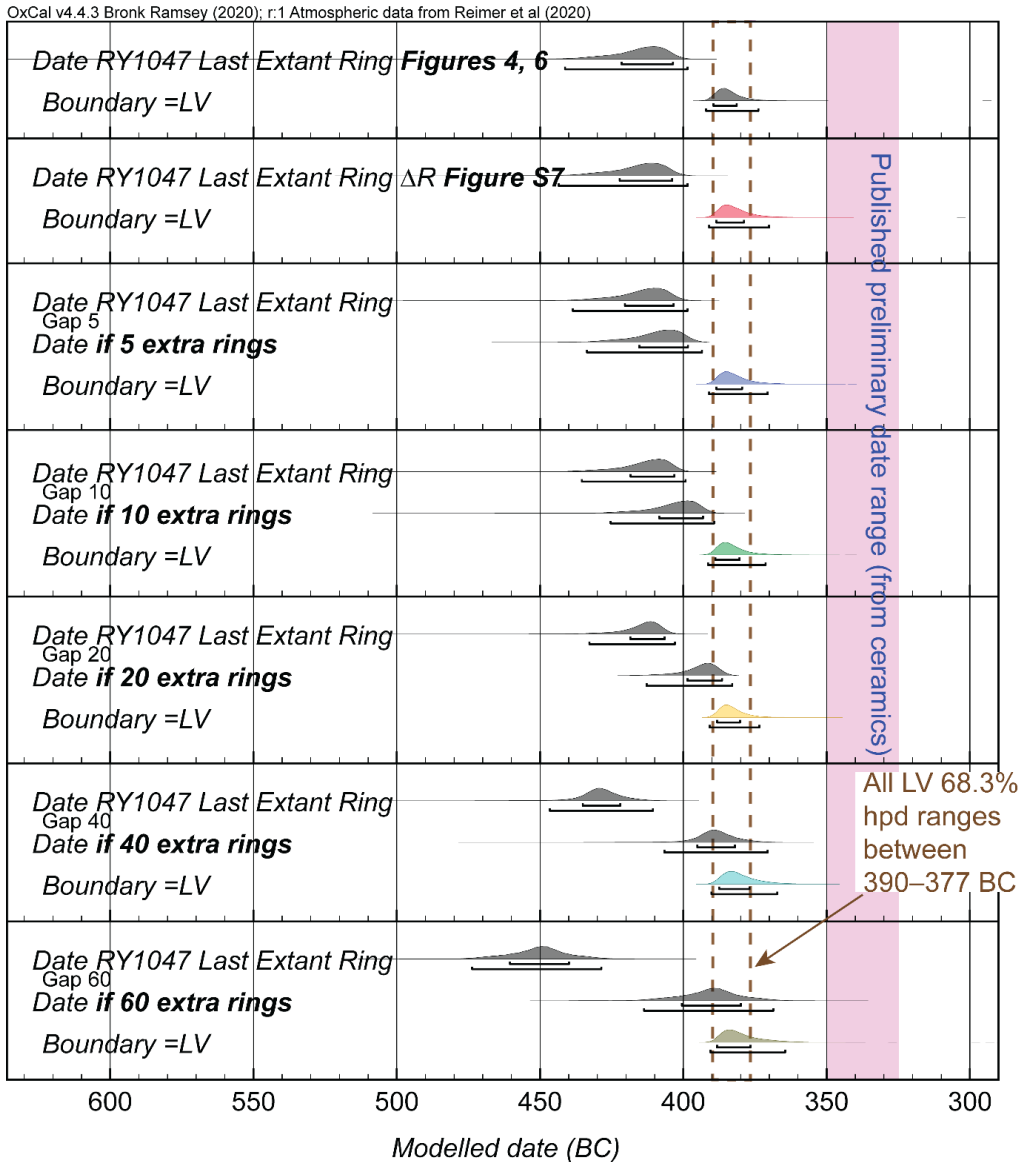


Figure S6. Range of some possible missing ring scenarios for W0056 to original waney edge/bark versus date for the LV. The LV Boundary is approximately stable under different scenarios. We show here models allowing for 0, 5, 10, 20, 40 or 60 missing rings after the last extant tree-ring on ship timber W0056. Note the models also allow for a possible small growing season radiocarbon offset as perhaps relevant to the two *Lamiaceae* twigs (figure: S. Manning).

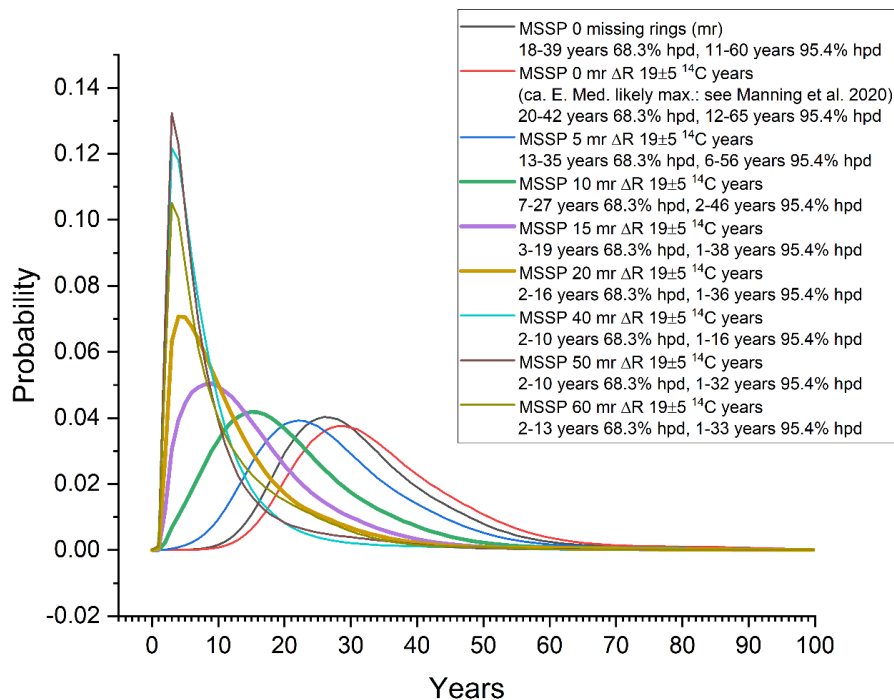


Figure S7. Maximum ship service periods (MSSP) under a range of scenarios from 0 to 60 assumed missing rings. The MSSP achieves a likely range of approximately 0–20 years once around 10–20 rings are assumed as missing (the 10, 15 and 20 missing rings models are shown highlighted with thicker lines) (figure: S. Manning).

#### Impact of growing season offset on $^{14}C$

It has been recently recognised that there is a small potential dating offset of up to around  $12 \pm 5$  to  $19 \pm 5$   $^{14}C$  years potentially relevant for East Mediterranean-Near Eastern plants with winter–spring or early summer growing seasons that are substantially different from those of the temperate trees providing the data for the IntCal  $^{14}C$  curves, whose growing seasons are from spring through summer (Manning *et al.* 2018, 2020). This is relevant especially to plants growing in warmer, more arid low altitude and low latitude Mediterranean ecological zones, and winter field crops like barley or wheat. In the Mazotos case, the timber is from a high-altitude tree species (*Pinus nigra*) whose spring-summer growing season is comparable to IntCal, while olive fruit grows through the summer and is only harvested in the autumn, again likely yielding an average  $^{14}C$  age compatible with IntCal. Only the Lamiaceae twigs might be an exception. While plants in this family exhibit plasticity in seasonal wood cell production, both cold winter temperatures and summer drought restrict their growing season (Camarero *et al.* 2013). Figure S8 shows the Figure 6b result re-run allowing for a plausible

maximum growing season offset ( $19 \pm 5$   $^{14}\text{C}$  years) applied to the two Lamiaceae sample dates—there is no substantive difference. Thus, this topic is not an issue in this case.

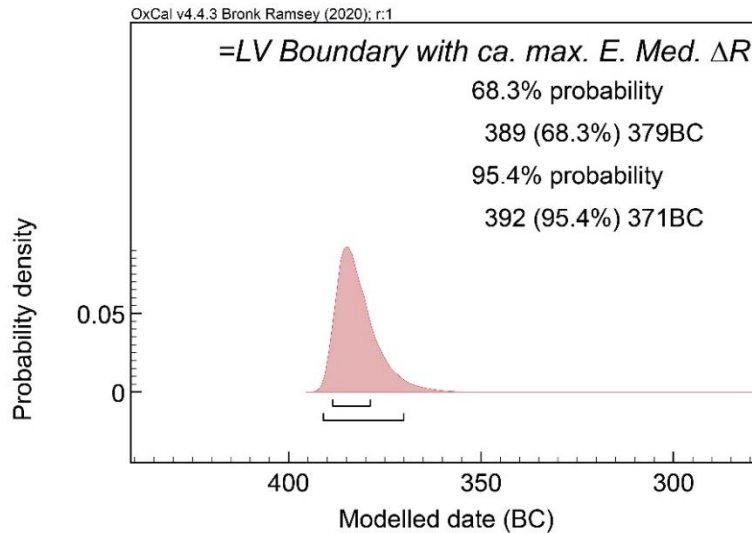


Figure S8. LV Boundary re-run if the likely maximum potential growing season offset ( $19 \pm 5$   $^{14}\text{C}$  years: see Manning et al. 2020) is applied to the samples (the Lamiaceae twigs) with potential growing season offsets, using the Figure 4 model (compare to the LV Boundary in Figure 6b). There is very little change in the dating estimates. Thus, this topic is not an issue for this particular dating case (figure: S. Manning).

### Radiocarbon dates and OxCal runfile

Details for the radiocarbon dates on the samples from the Mazotos shipwreck as employed in this study are set out in Table S1. The OxCal runfile for the model shown in Figure 4 is listed in Table S2. Dates on the olive pits were obtained from two laboratories (Oxford Radiocarbon Accelerator Unit, OxA and The Vienna Environmental Research Accelerator, VERA). The results from the two different laboratories are closely comparable, supporting their accuracy. The weighted average of the OxA data ( $n = 7$ ) is  $2297 \pm 11$   $^{14}\text{C}$  years BP and the weighted average of the VERA data ( $n = 4$ ) is  $2287 \pm 16$   $^{14}\text{C}$  years BP (Ward & Wilson 1978). All 11 data can be satisfactorily combined suggesting they reflect approximately the same radiocarbon age:  $2294 \pm 10$   $^{14}\text{C}$  years BP ( $\chi^2$  test,  $df=9$ ,  $T=10.2 < 16.9$ ) (Ward & Wilson 1978).

**Table S1. Mazotos  $^{14}\text{C}$  samples and their associated metadata. For details of the chemical pretreatment, target preparation and AMS measurement, see: for the VERA dates (Steier *et al.* 2004; Wild *et al.* 2008), and for the OxA dates (Bronk Ramsey *et al.* 2004; Brock *et al.* 2010). The VERA  $\delta^{13}\text{C}$  values were measured with the AMS system on the graphitised sample. The quoted OxA  $\delta^{13}\text{C}$  values were measured independently on a stable isotope mass spectrometer ( $\pm 0.3\text{‰}$  relative to VPDB). We thank both the Oxford Radiocarbon Accelerator Unit and the Vienna Environmental Research Accelerator (VERA) teams for the dates.**

Sample #	Lab ID	Description	Species	Tree-rings (relative years, RY)	$\delta^{13}\text{C}\text{‰}$	$^{14}\text{C}$ Age BP	SD
W0051-IV	VERA-6305	Twig from cargo dunnage (aft part of the hold)	Lamiaceae		$-30.0 \pm 0.8$	2299	29
W0051-VI	VERA-6306	Twig from cargo dunnage (aft part of the hold)	Lamiaceae		$-28.5 \pm 1.0$	2295	28
W0056/3 (MAZS-1/a)	VERA-6299B	Section of the ship's planking (stern, starboard)	<i>Pinus nigra</i>	1005-1007	$-28.9 \pm 0.8$	2367	28
W0056/3 (MAZS-1/b)	VERA-6300A	Section of the ship's planking (stern, starboard)	<i>Pinus nigra</i>	1008-1012	$-28.1 \pm 0.7$	2401	33
W0056/3 (MAZS-1/b)	VERA-6300B	Section of the ship's planking (stern, starboard)	<i>Pinus nigra</i>	1008-1012	$-26.7 \pm 0.6$	2403	33
W0056/3 (MAZS-1/c)	VERA-6301A	Section of the ship's planking (stern, starboard)	<i>Pinus nigra</i>	1023-1027	$-27.7 \pm 0.7$	2416	30
W0056/3 (MAZS-1/c)	VERA-6301B	Section of the ship's planking (stern, starboard)	<i>Pinus nigra</i>	1023-1027	$-26.3 \pm 0.8$	2395	30
W0056/3 (MAZS-1/d)	VERA-6302A	Section of the ship's planking (stern, starboard)	<i>Pinus nigra</i>	1033-1037	$-26.7 \pm 0.7$	2430	27

W0056/3 (MAZS-1/d)	VERA-6302B	Section of the ship's planking (stern, starboard)	<i>Pinus nigra</i>	1033-1037	-26.3±0.8	2394	30
W0056/3 (MAZS-1/e)	VERA-6303A	Section of the ship's planking (stern, starboard)	<i>Pinus nigra</i>	1038-1042	-26.4±0.8	2425	31
W0056/3 (MAZS-1/e)	VERA-6303B	Section of the ship's planking (stern, starboard)	<i>Pinus nigra</i>	1038-1042	-28.3±0.8	2415	29
W0056/3 (MAZS-1/f)	VERA-6304B	Section of the ship's planking (stern, starboard)	<i>Pinus nigra</i>	1043-1047	-26.9±1.0	2443	31
G0005i/a	VERA-6082a	Pit excavated in the bow area (Starboard)	<i>Olea europaea</i>		-24.6±1.9	2284	37
G0005i/b	VERA-6082b	Pit excavated in the bow area (Starboard)	<i>Olea europaea</i>		-24.7±1.2	2307	25
G0005i/c	VERA-6082c	Pit excavated in the bow area (Starboard)	<i>Olea europaea</i>		-23.5±1.3	2279	32
G0005i/d	VERA-6082d	Pit excavated in the bow area (Starboard)	<i>Olea europaea</i>		-25.2±1.6	2261	35
G0362i/a	OxA-31836	Pit found inside a Chian amphora stowed at the aft part of the hold	<i>Olea europaea</i>		-23.11±0.3	2246	26
G0362i/b	OxA-31877	Pit found inside a Chian amphora stowed at the aft part of the hold	<i>Olea europaea</i>		-23.69±0.3	2269	25
G0288i/a	OxA-32005	Pit excavated in the bow area (Starboard)	<i>Olea europaea</i>		-23.60±0.3	2306	25

G0288i/b	OxA-32006	Pit excavated in the bow area (Starboard)	<i>Olea europaea</i>		-21.65±0.3	2308	24
G0362/c	OxA-32794	Pit found inside a Chian amphora stowed at the aft part of the hold	<i>Olea europaea</i>		-23.22±0.3	2351	36
G0362/d	OxA-32795	Pit found inside a Chian amphora stowed at the aft part of the hold	<i>Olea europaea</i>		-23.60±0.3	2321	36
G0362/e	OxA-32796	Pit found inside a Chian amphora stowed at the aft part of the hold	<i>Olea europaea</i>		-25.86±0.3	2325	36

**Table S2. The OxCal (Bronk Ramsey 2009a) runfile for the Mazotos ship dating model shown in Figure 4. The model uses a higher ( $\times 100$ ) kIterations value than the OxCal default because sometimes runs of a default model do not achieve good convergence (all elements with Convergence values  $\geq 95$ ) due to the possible (very small) probability ambiguity in the third century BC (see Figure 4 where the dunnage and olive pit samples offer *non-modelled* dating probability in the third century BC). Use of a higher kIterations value usually avoids occasional poor convergence runs—however, note that this means the model takes longer to run than usual. The OxCal General Outlier model (Bronk Ramsey 2009b) is applied to the dates on short-lived samples and the OxCal SSimple Outlier model (Bronk Ramsey 2009b) is applied to the dates in the wiggle-match (Bronk Ramsey *et al.* 2001).**

```
Options()
{
  Resolution=1;
  kIterations=3000;
};
Plot( )
{
  Outlier_Model("General",T(5),U(0,4),"t");
  Outlier_Model("SSimple",N(0,2),0,"s");
  D_Sequence("W0056 Pinus nigra plank from stern area")
  {
    R_Date("VERA-6299B MAZS-1 W0056/3 RY1005-1007",2367,28)
    {
      Outlier ("SSimple",0.05);
      color="magenta";
    };
    Gap(4);
    R_Combine("MAZS-1 RY1008-1012")
    {
      Outlier("SSimple",0.05);
      color="magenta";
      R_Date("VERA-6300A MAZS-1 W0056/3 RY1008-1012",2401,33)
```

```

{
  Outlier ("SSimple",0.05);
};
R_Date("VERA-6300B MAZS-1 W0056/3 RY1008-1012",2403,33)
{
  Outlier ("SSimple",0.05);
};
};
Gap(15);
R_Combine("MAZS-1 RY1023-1027")
{
  Outlier("SSimple",0.05);
  color="magenta";
  R_Date("VERA-6301A MAZS-1 W0056/3 RY1023-1027",2416,30)
  {
    Outlier ("SSimple",0.05);
  };
  R_Date("VERA-6301B MAZS-1 W0056/3 RY1023-1027",2395,30)
  {
    Outlier ("SSimple",0.05);
  };
};
Gap(10);
R_Combine("MAZS-1 RY1033-1037")
{
  Outlier("SSimple",0.05);
  color="magenta";
  R_Date("VERA-6302A MAZS-1 W0056/3 RY1033-1037",2430,27)
  {
    Outlier ("SSimple",0.05);
  };
  R_Date("VERA-6302B MAZS-1 W0056/3 RY1033-1037",2394,30)
  {
    Outlier ("SSimple",0.05);
  };
};

```

```

};
};
Gap(5);
R_Combine("MAZS-1 RY1038-1042")
{
  Outlier("SSimple",0.05);
  color="magenta";
  R_Date("VERA-6303A MAZS-1 W0056/3 RY1038-1042",2425,31)
  {
    Outlier ("SSimple",0.05);
  };
  R_Date("VERA-6303B MAZS-1 W0056/3 RY1038-1042",2415,29)
  {
    Outlier ("SSimple",0.05);
  };
};
};
Gap(5);
R_Date("VERA-6304B MAZS-1 W0056/3 RY1043-1047",2443,31)
{
  Outlier ("SSimple",0.05);
  color="magenta";
};
};
Gap(2);
Date("Date RY1047 Last Extant Ring");
};
Phase("Period around and to LV")
{
  Sequence("Ship TPQ to LV from dunnage")
  {
    Boundary("=Date RY1047 Last Extant Ring");
    Phase ("Dunnage and LV Date")
    {
      R_Date("VERA-6305 W0051-IV 4yrs growth",2299,29)
      {

```

```
Outlier ("General",0.05);
color="green";
};
R_Date("VERA-6306 W0051-VI 5yrs growth",2295,28)
```

```
{
  Outlier ("General",0.05);
  color="green";
};
};
```

```
Interval(N(1.75,0.25));
```

```
Boundary("LV");
```

//14C dated mid-point to exterior minimum interval is 2 or c. 1.5 years from dunnage samples and date for cutting dunnage likely LV year within 1 year, like olives, so effectively the same date.

```
};
```

```
Sequence("LV date from olives on board ship")
```

```
{
```

```
Tau_Boundary ("T");
```

```
Phase("Contents Ship Last Voyage – Olive Pits from storage jars")
```

```
{
```

```
R_Date("OxA-31836 G0362i NM0435 ESEA 215/12 Olea europaea pit",2246,26)
```

```
{
```

```
Outlier ("General",0.05);
```

```
color="orange";
```

```
};
```

```
R_Date("OxA-31877 G0362i NM0435 ESEA 215/12 Olea europaea pit",2269,25)
```

```
{
```

```
Outlier ("General",0.05);
```

```
color="orange";
```

```
};
```

```
R_Date("OxA-32005 G0288i NM0080 ESEA 66/10 Olea europaea pit", 2306,25)
```

```
{
```

```
Outlier ("General",0.05);
```

```
color="orange";
```

```

};
R_Date("OxA-32006 G0288i NM0080 ESEA 66/10 Olea europaea pit", 2308,24)
{
  Outlier ("General",0.05);
  color="orange";
};
R_Date("OxA-32794 G0362 NM435 PO488_1 Olea europaea pit",2351,36)
{
  Outlier ("General",0.05);
  color="orange";
};
R_Date("OxA-32795 G0362 NM435 PO488_2 Olea europaea pit",2321,36)
{
  Outlier ("General",0.05);
  color="orange";
};
R_Date("OxA-32796 G0362 NM435 PO488_3 Olea europaea pit",2325,36)
{
  Outlier ("General",0.05);
  color="orange";
};
R_Date("VERA-6082a G005i NM0187 ESEA 86/4 Olea europaea pit",2284,37)
{
  Outlier ("General",0.05);
  color="orange";
};
R_Date("VERA-6082b G005i NM0187 ESEA 86/4 Olea europaea pit",2307,25)
{
  Outlier ("General",0.05);
  color="orange";
};
R_Date("VERA-6082c G005i NM0187 ESEA 86/4 Olea europaea pit",2279,32)
{
  Outlier ("General",0.05);

```

```
color="orange";
};
R_Date("VERA-6082d G005i NM0187 ESEA 86/4 Olea europaea pit",2261,35)
{
  Outlier ("General",0.05);
  color="orange";
};
};
Boundary("=LV");
};
};
Tau=(LV-T);
Difference("SPMax","LV","Date RY1047 Last Extant Ring");
};
```

## References

- BERNABEI, M. *et al.* 2019. Dendrochronological evidence for long-distance timber trading in the Roman Empire. *PLoS ONE* 14: e0224077. <https://doi.org/10.1371/journal.pone.0224077>
- BROCK, F., T.F.G. HIGHAM, P. DITCHFIELD & C. BRONK RAMSEY. 2010. Current pretreatment methods for AMS radiocarbon dating at the Oxford Radiocarbon Accelerator Unit (ORAU). *Radiocarbon* 52: 103–12. <https://doi.org/10.1017/S0033822200045069>
- BRONK RAMSEY, C. 2009a. Bayesian analysis of radiocarbon dates. *Radiocarbon* 51: 337–60. <https://doi.org/10.1017/S0033822200033865>
- 2009b. Dealing with outliers and offsets in radiocarbon dating. *Radiocarbon* 51: 1023–45. <https://doi.org/10.1017/S0033822200034093>
- BRONK RAMSEY, C., T. HIGHAM & P. LEACH. 2004. Towards high-precision AMS: progress and limitations. *Radiocarbon* 46: 17–24. <https://doi.org/10.1017/S0033822200039308>
- BRONK RAMSEY, C., J. VAN DER PLICHT & B. WENINGER. 2001. ‘Wiggle matching’ radiocarbon dates. *Radiocarbon* 43: 381–89. <https://doi.org/10.1017/S0033822200038248>
- BÜNTGEN, U. *et al.* 2006. 700 years of settlement and building history in the Lössental/Switzerland. *Erdkunde* 60: 96–112. <https://doi.org/10.3112/erdkunde.2006.02.02>
- CAMARERO, J.J., S. PALACIO & G. MONTSERRAT-MARTI. 2013. Contrasting seasonal overlaps between primary and secondary growth are linked to wood anatomy in Mediterranean subshrubs. *Plant Biology* 15: 798–807. <https://doi.org/10.1111/j.1438-8677.2012.00702.x>
- CRONE, A. & C.M. MILLS. 2012. Timber in Scottish buildings, 1450–1800: a dendrochronological perspective. *Proceedings of the Society of Antiquaries of Scotland* 142: 329–69.
- DODDS, J. & J. MOORE. 2005. *Building the wooden fighting ship*. London: Chatham.
- ECKSTEIN, D. 2007. Human time in tree rings. *Dendrochronologia* 24: 53–60. <https://doi.org/10.1016/j.dendro.2006.10.001>
- KUNIHOLM, P.I. & C.L. STRIKER. 1987. Dendrochronological investigations in the Aegean and neighboring regions, 1983–1986. *Journal of Field Archaeology* 14: 385–98. <https://doi.org/10.1179/jfa.1987.14.4.385>
- LORENTZEN, B., S.W. MANNING, D. CVIKEL & Y. KAHANOV. 2014a. High-precision dating the Akko 1 shipwreck, Israel: wiggle-matching the life and death of a ship into the historical record. *Journal of Archaeological Science* 41: 772–83. <https://doi.org/10.1016/j.jas.2013.10.013>

- LORENTZEN, B., S.W. MANNING & Y. KAHANOV. 2014. The 1<sup>st</sup> millennium AD Mediterranean shipbuilding transition at Dor/Tantura Lagoon, Israel: dating the Dor 2001/1 shipwreck. *Radiocarbon* 56: 667–78. <https://doi.org/10.2458/56.17445>
- MANNING, S.W. *et al.* 2009. Absolute age of the Uluburun shipwreck: a key Late Bronze Age time-capsule for the East Mediterranean, in S.W. Manning & M.J. Bruce (ed.) *Tree-rings, kings and Old World archaeology and environment: papers presented in honor of Peter Ian Kuniholm*: 163–87. Oxford: Oxbow.
- 2018. Fluctuating radiocarbon offsets observed in the Southern Levant and implications for archaeological chronology debates. *Proceedings of the National Academy of Sciences of the USA* 115: 6141–46. <https://doi.org/10.1073/pnas.1719420115>
- 2020. Mediterranean radiocarbon offsets and calendar dates for prehistory. *Science Advances* 6: eaaz1096. <https://doi.org/10.1126/sciadv.aaz1096>
- MEIGGS, R. 1982. *Trees and timber in the ancient Mediterranean world*. Oxford: Clarendon.
- MILES, D. 2006. Refinements in the interpretation of tree-ring dates for oak building timbers in England and Wales. *Vernacular Architecture* 37: 84–96. <https://doi.org/10.1179/174962906X158291>
- POMEY, P. & E. RIETH. 2005. *L'archéologie navale*. Paris: Editions Errance.
- STEIER P. *et al.* 2004. Pushing the precision of <sup>14</sup>C measurements with AMS. *Radiocarbon* 46: 5–16. <https://doi.org/10.1017/S0033822200039291>
- WARD, G.K. & S.R. WILSON. 1978. Procedures for comparing and combining radiocarbon age determinations: a critique. *Archaeometry* 20: 19–31. <https://doi.org/10.1111/j.1475-4754.1978.tb00208.x>
- WILD, E.M. *et al.* 2008. <sup>14</sup>C dating of the Upper Paleolithic site at Krems-Hundssteig in Lower Austria. *Radiocarbon* 50: 1–10. <https://doi.org/10.1017/S0033822200043332>